

# Design of a rugged 308 nm tunable UV laser for airborne LIF measurements on top of Zeppelin NT

M. Strotkamp<sup>\*a</sup>, A. Munk<sup>a</sup>, B. Jungbluth<sup>a</sup>, K. Dahlhoff<sup>b</sup>, P. Jansen<sup>b</sup>, S. Broch<sup>c</sup>, S. Gomm<sup>c</sup>, M. Bachner<sup>c</sup>, H. Fuchs<sup>c</sup>, F. Holland<sup>c</sup>, A. Hofzumahaus<sup>c</sup>

<sup>a</sup>Fraunhofer Institute for Laser Technology (ILT), Steinbachstr. 15, 52074 Aachen, Germany;

<sup>b</sup>Central Institute of Engineering, Electronics and Analytics (ZEA-1), Forschungszentrum Jülich

GmbH, 52425 Jülich, Germany; <sup>c</sup>Institute for Energy and Climate Research: Troposphere (IEK-8),

Forschungszentrum Jülich GmbH, 52425 Jülich, Germany

## ABSTRACT

In this work, a detailed analysis and redesign of a tunable UV laser is presented. The laser is part of measurement system of "IEK 8, Forschungszentrum Jülich" for airborne LIF analysis of the OH-radical concentration. The design concept of the laser comprises a frequency doubled Nd:YAG laser as pump source, a dye as active medium to emit light at 616 nm, and a NLO crystal as intracavity frequency doubler. The output wavelength is tunable by a combination of dispersion prisms and an etalon.

During measurement campaigns, the laser is mounted on top of Zeppelin NT and therefore is exposed to temperatures ranging from 10 to 40 °C and ambient pressures from 800 to 1000 hPa. In former flights the output power of an existing laser decreased rapidly and the wavelength was unstable during the flights and therefore hinders continuous measurements.

The analysis of the existing laser combines a theoretical study of tolerance requirements with experimental testing of opto-mechanical components and of the entire laser system in a climatic test chamber. The performance of the laser is measured over the expected temperature range. It is shown that changing the baseplate temperature by a few Kelvin stops laser emission completely. The optical mounts that are used in the laser and worthwhile alternatives were tested separately in the climatic chamber. The stability of the best mounts exceeds those currently used by a factor of 50.

A new laser has been built based on the results of the analysis and further experiments for an optical redesign. This laser was on a field campaign for several weeks and worked reliably.

**Keywords:** airborne, UV laser, tunable, dye laser, analysis

## 1. INTRODUCTION

Most of the chemical processes that are relevant for the air quality and climate change take place in the atmospheric boundary layer in a height from one to two kilometers. For a detailed forecast of short and long term changes in the chemical composition of our atmosphere, a detailed knowledge of the relevant processes is essential. The free radicals and especially the Hydroxyl (OH) radical play an important role because they are involved in many chemical reactions and initiate the chemical breakdown of tropospheric trace gases such as CO, SO<sub>2</sub>, NO<sub>x</sub>, CH<sub>4</sub> and other volatile organic compounds. The detection of Hydroxyl is challenging because of its high reactivity and the small atmospheric concentrations (typically ~ 10<sup>6</sup> molec. cm<sup>-3</sup>). A method with a sufficient sensitivity and accuracy for the measurement of such small concentrations is the Laser-Induced Fluorescence (LIF) technique [1].

The knowledge of the concentration and distribution of Hydroxyl within the atmosphere is of great importance for the climate research and especially for the smog forecast. As part of the project PEGASOS (Pan-European Gas-AeroSOI-climate Interaction Study) [2] that is funded by the EU, field campaigns with measurement on board of the Zeppelin NT took place over the Netherlands and northern Italy in summer 2012. Therefore, the laser has to meet the requirements of a LIF measurement under the conditions of a zeppelin flight and a daily continuously operation over several weeks without maintenance.

\*michael.strotkamp @ilt.fraunhofer.de; phone 49 241 8906-132; fax 49 241 8906-121; ilt.fraunhofer.de

The measurement on board of Zeppelin NT has several advantages over an airplane. Unlike an airplane the airship can stay at a fixed position or rise vertically. Hence it can measure height profiles or drift with the surrounding air mass to measure in-situ the development of the concentration of Hydroxyl over the time. A detailed description of the Zeppelin NT as a platform for atmospheric research can be found in [3].

For the LIF measurement of the OH concentration a laser with a wavelength of 308 nm, a tuning range of 100 GHz, and a power of 100 mW is needed. The linewidth of the laser has to be smaller than 7 GHz and the wavelength stability better than 1 pm to resolve the Doppler-broadening of the resonance line of OH. With a pulse repetition rate of 8.5 kHz and a pulse duration shorter than 30 ns and hence much shorter than the fluorescent lifetime of OH (200 -500 ns), a good signal to noise aspect is reached. During the measurement on the zeppelin the laser is exposed to temperatures ranging from 10 to 40 °C and ambient pressures from 800 to 1000 hPa. Within these ranges all requirements have to be fulfilled.

In the past mostly frequency doubled dye lasers that are pumped by frequency doubled Nd:YAG or Nd:YLF laser were used for airborne LIF measurements of OH concentrations [4] [5]. These measurements were performed on an airplane with different conditions concerning temperature and pressure. Laser based on this concept achieve high efficiencies but suffer from fluctuations of the output power [6] due to the complex and thereby susceptible setup. In addition to the intracavity frequency doubled dye laser there are also externally frequency doubled lasers with similar output power [7].

## 2. ANALYSIS OF THE PREVIOUS LASER SETUP

The analysis mainly consists of two parts, namely a theoretical tolerance analysis of the laser design and an experimental analysis of the laser susceptibility to temperature fluctuations, containing analyses of the single components and the entire setup as well.

### 2.1 Design of the previous laser setup

The optical system of the entire laser setup is mainly composed of four functional units: firstly the pump laser, secondly the beam shaping and delivery to the dye laser resonator (furthermore named pump optics), thirdly the dye laser resonator itself, including an internal frequency doubling unit and finally the beam shaping and delivery to the fiber coupled measurement cells (furthermore named fiber coupling).

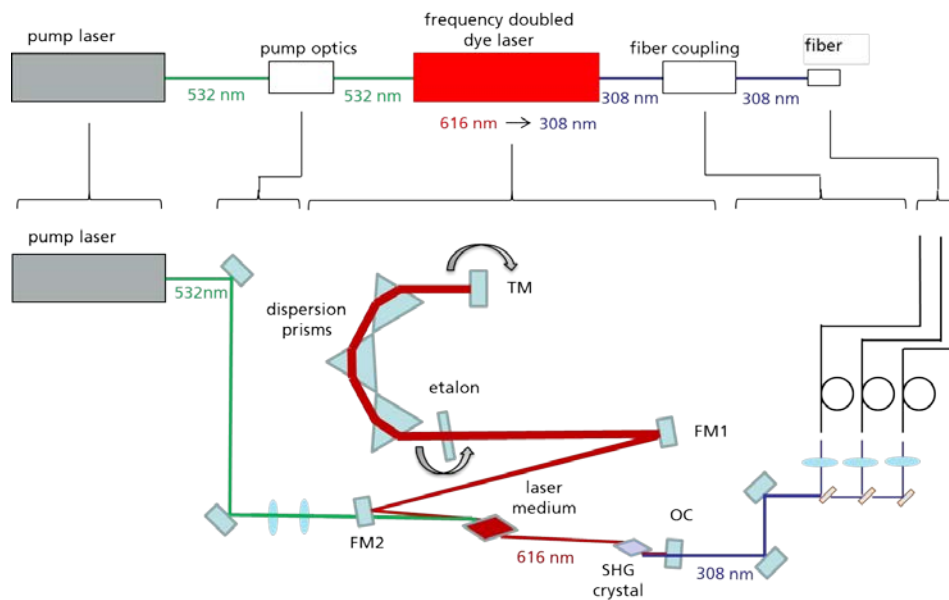


Figure 1. Setup of the laser.

Figure 1 presents a block diagram of the laser transmitter and a detailed sketch including all relevant optical elements in the beam path. The pump laser is a frequency doubled, diode pumped, q-switched Nd:YAG Laser (Spectra Physics, Navigator) emitting at 532 nm. The pump optics comprise of two 90° deflection mirrors and two lenses plus the dichroic input mirror of the resonator acting as a negative lens for the pump light. The tunable dye laser (New Laser Generation, Tintura) consists of a telescopic resonator containing three dispersive Brewster prisms and an air spaced etalon as wavelength filter, a dye cell with Rhodamin 101 solved in ethanol and an SHG unit with a Brewster-cut NLO crystal for type I phase-matching frequency doubling the dye laser wavelength from 616 nm to 308 nm in the UV. The laser box is hermetically sealed and filled with helium to reduce the pressure-dependence. The frequency doubled dye laser output is deflected by two 90° mirrors and split into three fraction of different power and finally focused independently into three multimode fibers, delivering the UV light to three different cells for referencing and measuring purpose, respectively.

## 2.2 Theoretical analysis

The tolerance analysis of the laser system is conducted analytically, assuming Gaussian beams and a paraxial optical system.

### Theoretical Basics

The tolerance analysis is carried out by a 3x3 matrix formalism as described e.g. in [8]. Here the well-known 2x2 matrix describing the ray transfer through a well-aligned, paraxial optical element or system, given by the matrix elements  $A$ ,  $B$ ,  $C$  and  $D$ , is expanded by two further matrix entries  $E$  and  $F$

$$\mathbf{M} = \begin{pmatrix} A & B & E \\ C & D & F \\ 0 & 0 & 1 \end{pmatrix} \quad (1)$$

where  $E$  and  $F$  give the output displacement  $h_{out}$  and tilt  $\theta_{out}$  of a reference input beam entering the optical element or system on the optical axis collinearly,  $h_{in} = \theta_{in} = 0$ .

For misaligned optical systems used in a single pass, the analysis is straight forward: Firstly, one has to define the 3x3 matrix  $\mathbf{M}_i$  for every single optical element. Here, the matrix entries  $E_i$  and  $F_i$  are functions of the displacement  $\Delta_i$  and tilt  $\delta_i$  of element  $i$  compared to a well-aligned situation. Secondly, one can derive the transfer matrix  $\mathbf{M}_S$  for the overall misaligned system by matrix multiplication of all  $\mathbf{M}_i$ . Finally, one find the displacement and tilt of the out beam  $h_{S,out}$  and tilt  $\theta_{S,out}$  as a function of the tilt and displacement of the input beam  $h_{S,in}$  and tilt  $\theta_{S,in}$  and the misalignment of the optical system  $\mathbf{\Delta} = \{\Delta_i\}$ ,  $\mathbf{\delta} = \{\delta_i\}$ .

$$\begin{aligned} h_{S,out} &= A_S \cdot h_{S,in} + B_S \cdot \theta_{S,in} + E_S \\ \theta_{S,out} &= C_S \cdot h_{S,in} + D_S \cdot \theta_{S,in} + F_S \end{aligned} \quad (2)$$

For misaligned periodic systems or resonators one can define an Eigenproblem for the orientation  $(h_E, \theta_E)$  of its beam axis according to the optical axis of the well-aligned resonator by the means of the roundtrip matrix  $\mathbf{M}_R$

$$\begin{pmatrix} h_E \\ \theta_E \\ 1 \end{pmatrix} = \begin{pmatrix} A_R & B_R & E_R \\ C_R & D_R & F_R \\ 0 & 0 & 1 \end{pmatrix} \cdot \begin{pmatrix} h_E \\ \theta_E \\ 1 \end{pmatrix} \quad (3)$$

The Eigenproblem for the  $q$ -parameter of a Gaussian beam reproducing itself after a complete resonator roundtrip and the definition of the  $q$ -parameter itself are presumed to remain unchanged by the misalignment of the system

$$q_E = \frac{A_R \cdot q_E + B_R}{C_R \cdot q_E + D_R} \quad (4)$$

$$q = z + z_R, \quad z_R = \frac{\pi \cdot w_0^2}{\lambda} \quad (5)$$

where  $z_R$  is the Rayleigh length of the Gaussian beam with a waist radius  $w_0$ .

The changed beam path of the Eigenmode inside the resonator worsens the laser performance basically by three effects. Firstly by a reduced laser gain due to a smaller spatial overlap of the Eigenmode with the pumped volume inside the laser medium, secondly by higher roundtrip losses due to beam clipping at apertures and thirdly by a reduced conversion efficiency due to the phase mismatch resulting from a tilt of the laser beam inside the SHG crystal.

For collimated, collinear, Gaussian shaped beams the reduction of the logarithmic small signal gain  $\ln G_0$  by a smaller overlap of pump and laser mode can be described as

$$\ln G_0 = \ln G_{0,\max} \cdot \prod_{\psi=x,y} \exp\left(-2 \frac{b_{\psi}^2}{1 + a_{\psi}^2}\right) \quad (5)$$

$$\text{with } a_{x/y} = \frac{w_{x/y}}{w_{\text{pump},x/y}} \quad \text{and} \quad b_{x/y} = \frac{h_{E,x/y}}{w_{\text{pump},x/y}}$$

where  $a_{x,y}$  and  $b_{x,y}$  indicate normalized laser mode radius  $w$  and beam displacement  $h_E$  inside the gain medium in multiples of the pump beam radius  $w_{\text{pump}}$  for  $x$ - and  $y$ -direction perpendicular to the beam direction  $z$ .

The reduced conversion efficiency of the intracavity SHG for an angular misalignment of the laser mode due to the phase matching direction is calculated in plane wave, fixed field approximation [9], yielding

$$\eta = \eta_{\max} \cdot \text{sinc}^2(\pi \cdot \theta_E / 2 \cdot \Theta_{\text{NLO-crystal}}) \quad (6)$$

where  $\Theta_{\text{NLO-crystal}}$  indicates the angular tolerance of the NLO crystal, defined as the angle where the phase-mismatch over the entire crystal length reaches  $\pi$ , and  $\theta_E$  is the tilt of the laser Eigenmode inside the crystal.

For the actual dye laser cavity losses due to clipping can be neglected, because the aperture widths of all resonator optics are much larger than the beam width and beam displacements.

### System Analysis

The tolerance analysis of the laser is split into three parts: Firstly, the reduction of dye laser gain due to power fluctuation and beam pointing of the pump laser and due to misalignments of the pump optics. Secondly, the reduction of dye laser gain, SHG conversion efficiency and wavelength shift due to the misalignment of the dye laser cavity. Thirdly, reduced coupling efficiency into the fiber coupled measurement cells due to the beam pointing of the dye laser and misaligned fiber coupling optics.

As a result of the analysis one finds that the misalignment of the dye laser cavity has by far the strongest effect. The principal plane of the NLO crystal coincides with the sagittal plane of the resonator. Therefore, misalignments within the sagittal plane are more serious than those in the tangential plane. As seen in Figure 2 the folding mirror 1 and tuning mirror are the most critical components inside the resonator. A tilt in the sagittal plane of only 40  $\mu\text{rad}$  and 20  $\mu\text{rad}$ , respectively, reduces the calculated laser power to zero. For the folding mirrors 1 and 2 with curved surfaces also displacements are critical. The laser operation already extinguishes for a small displacement of these mirrors in the order of about 5  $\mu\text{m}$  within the sagittal plane.

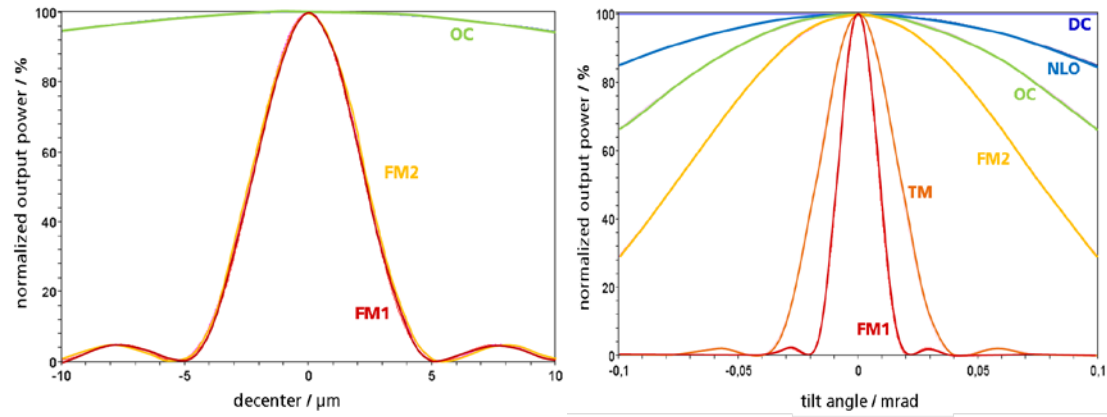


Figure 2. Influence of a displacement (left) and tilt (right) of an optical element on the laser power.

Compared to the high sensitivity of the cavity optics, the influence of misaligned pump optics on the dye laser power is much smaller. Misalignments of the pump optics in the order of 5  $\mu\text{m}$  or 20  $\mu\text{rad}$  as discussed above for critical cavity optics reduce the dye laser power by not more than 2%. The coupling of the dye laser output into the high order multimode fiber is even less critical than that.

Table 1. Influence of optics misalignment on the Eigenmode position in the dye laser cavity.

misalignment			beam displacement*		beam tilt**
optics	$\Delta/\text{mm}$	$\delta/\text{mrad}$	$h_{E,x}/\text{mm}$	$h_{E,y}/\text{mm}$	$\theta_{E,y}/\text{mrad}$
FM 1		1	2,0	4,3	21,7
	1		8,1	17,1	86,8
FM 2		1	0,3	0,5	2,5
	1		8,6	16,6	84,5
OC		1	0,1	0,3	1,5
	1		0,3	1,2	6,1
TM		1	1,0	2,1	10,9
DC		1	0,003	0,004	0,02
NLO		1	0,001	0,003	0,6

\* in the dye cell (DC), \*\* in the NLO-Xtal

### 2.3 Components testing

The stability of the mirror mounts currently used in the laser system and several alternatives was tested in a climatic test chamber under ambient conditions expected during a flight on the zeppelin. The temperature ranges from 10  $^{\circ}\text{C}$  to 40  $^{\circ}\text{C}$ , the rate of change was 15  $^{\circ}\text{C}$  per hour, a whole cycle took five and a half hours and with every mount at least three cycles were carried out. The resulting tilts of the tested mirror mounts to the baseplate in the horizontal and vertical direction were monitored online with an autocollimator.

The temperature and tilt of the mirror mount currently used in the resonator are shown on the left side of Figure 3. The measured tilt results from superposition of three different effects, namely of a setting at the beginning of the first temperature cycle, a cyclically tilt with the temperature and a drift i.e. a hysteresis after a complete temperature cycle. The setting at the beginning in the horizontal direction is greater than in the vertical direction. In additional tests it was shown that the setting at the beginning occurs after the mounting on the baseplate and the installation of the mirror but not after the adjustment with the screws. The cyclically tilt on the other hand is eight times greater in the vertical direction. For both directions the drift becomes smaller after each cycle and asymptotically reaches a final position. On the right side of Figure 3 the same test is shown for an alternative mount. There is no setting or drift and the amplitude of the cyclically tilt is 50 times smaller.

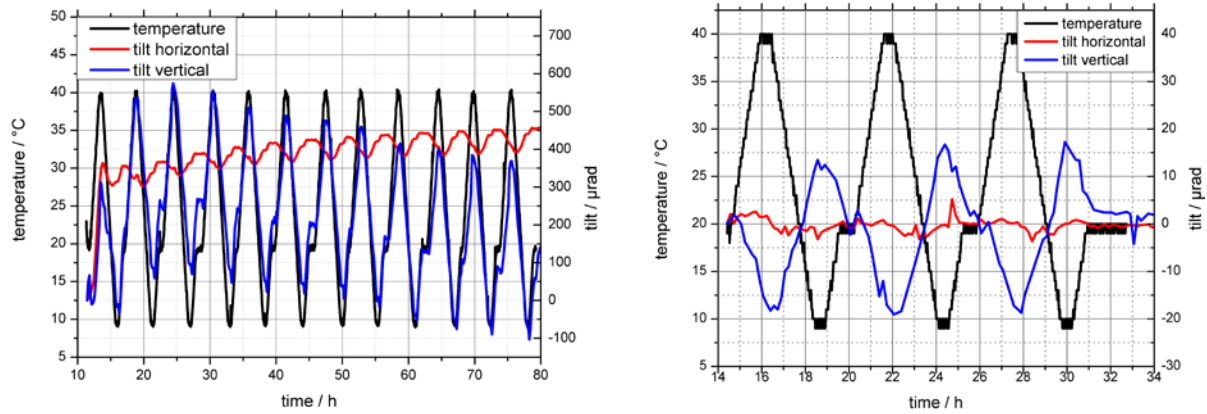


Figure 3. Test of the currently in the resonator used and the most stable mirror mounts with the tilt and temperature.

The results of the tests with all currently used and alternative mounts are listed in Table 2. It is shown that the mounts that are used for the resonator are the most susceptible to misalignment with temperature changes. The flexure mounts are less susceptible compared with the kinematic mounts. But even the most stable mount tested does not match the requirement of the most critical component of the resonator.

Table 2. Results of the tests in the climatic test chamber for all tested mirror mounts. The cyclically tilt, setting and drift in horizontal and vertical direction are given in  $\mu\text{rad}$ . Two values for the drift are given for the first and last cycle if necessary.

usage	type	material kind	horizontal tilt	vertical tilt	horizontal setting	vertical setting	horizontal drift	vertical drift
deflection	1" Center Mount	aluminium kinematic	40	90	65	65	5 / 0 *	0 *
NLO oven	Blank Plate	aluminium kinematic	25	60	25	10	0	0
resonator	0.5" Corner Mount	aluminium kinematic	60	475	300	225	25 / 5 *	+100 / -30 *
alternative #1	1" Center Mount	brass flexure	5	35	0	0	0	0
alternative #2	1" Center Mount	stainless steel flexure	35	40	0	5	0	10 / 0
alternative #3	0.5" Center Mount	stainless steel flexure	50	45	0	10	0	0
alternative #4	1" Center Mount	stainless steel kinematic	70	90	10	20	-10	0
alternative #5	1" Center Mount	stainless steel kinematic	30	30	10	0	30 / 20	0
alternative #6	0.5" Center Mount	aluminium kinematic	80	70	0	70	50 / 30	80 / 40

\* 12 instead of 3 cycles

## 2.4 Laser performance

The performance of the pump laser and the whole laser system was tested in the climatic test chamber as well. The development of the output power and the pointing of the pump laser with a change of the ambient temperature is shown in Figure 4. The output power decreases over 20 % with rising temperature and rises again at lower temperatures. There is no hysteresis for the power and a second test confirms the results. The pointing of the pump laser changes five times stronger in the vertical than in the horizontal direction but is within the specification of the manufacturer. The pointing shows a hysteresis after a whole temperature cycle.

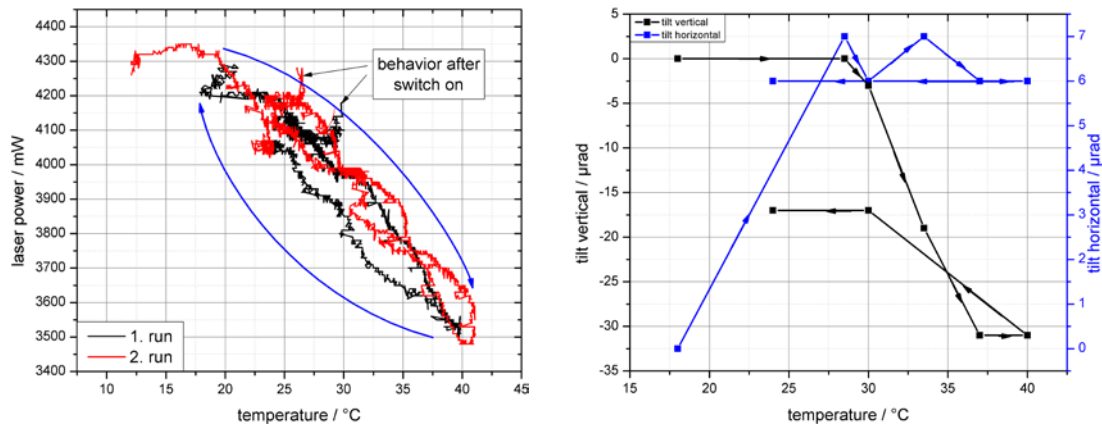


Figure 4. Development of output power (left) and pointing (right) of the pump laser with the temperature.

On the left side of Figure 5 the output power of the UV laser in dependence on the temperature is shown. First the temperature was increased from 25 °C to 40 °C and the laser power falls from 170 mW to 20 mW. The analysis of the beam profiles shows that the laser develops higher modes for higher temperatures. At 25 °C the beam profile shows a TEM<sub>00</sub>, for 30 °C it becomes a TEM<sub>10</sub> and for 40 °C it shows a TEM<sub>20</sub>. Additionally the beam profiles show that only the fraction of the mode is converted to the UV that meets the critical angle of the NLO crystal. After lowering the temperature to 25 °C again the laser has only 80 mW and the beam profile still shows a TEM<sub>20</sub>. An adjustment of the critical angle of the NLO crystal shows no effect. But after a realignment of the pump mirror the laser has an output power of 170 mW and a TEM<sub>00</sub> again. After the temperature was decreased to 15 °C the output power falls to 50 mW and it only increased to 110 mW when the temperature was back to 25 °C. A realignment of the NLO crystal and the pump mirror increased the power to 170 mW again.

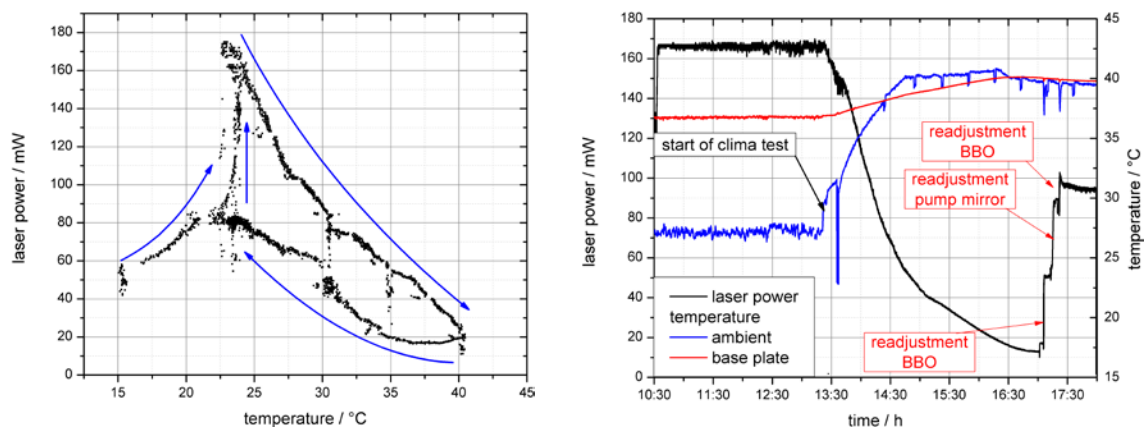


Figure 5. Dependence of the laser output power on the temperature (left) and development of output power, baseplate and ambient temperature with the time (right).

On the right side of Figure 5 the output power of the UV laser, the ambient temperature and the temperature of the resonator baseplate is shown. The laser runs for three hours at 27 °C without major fluctuations of the output power of 170 mW before the ambient temperature is risen to 40 °C within 90 minutes. The temperature of the baseplate rises another two hours until it stabilizes at 40 °C. The output power of the laser decreases to 10 mW until the temperature of the baseplate is stabilized. A readjustment of the NLO crystal increased the power to 50 mW, a following readjustment of the pump mirror increased it to 90 mW and a final readjustment of the NLO crystal increased it to 100 mW. The initial power is not reached because the resonator is probably misaligned.

### 3. REDESIGN OF THE LASER

Based on the results of the theoretical and experimental analysis and additional tests a laser with a stiffer mechanical setup was designed at “ZEA-1” including first improvements of the optical design.

### 3.1 Improved setup

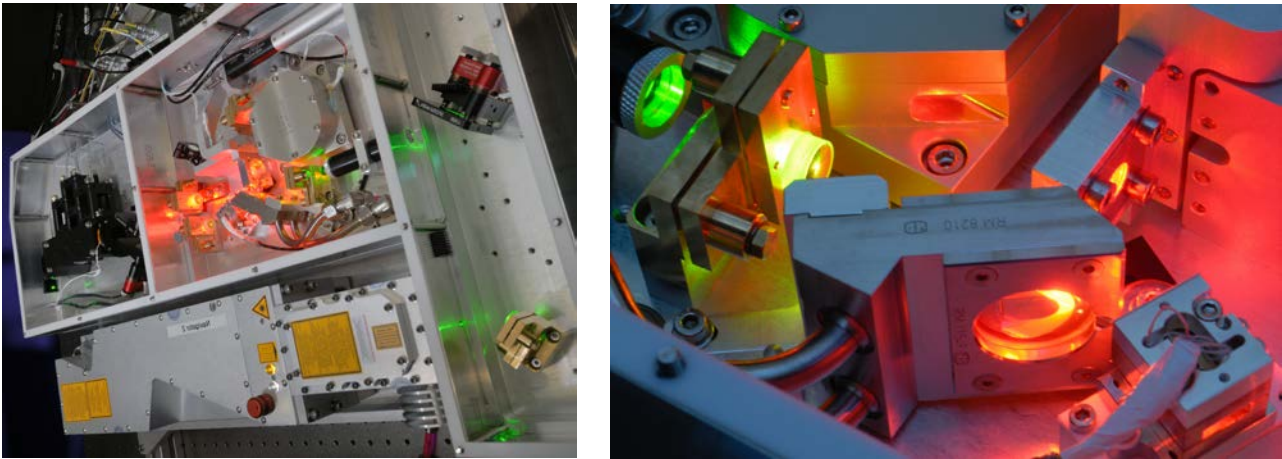


Figure 6. Setup of the new laser in an overview (left) and a detailed view of the resonator (right).

The improved setup includes a new baseplate with an improved mechanical stability and is heated to 40 °C. The distance between the pump laser and the resonator is reduced by 20 % in order to mitigate the susceptibility to a changing of the pointing of the pump laser. All mirror mounts were replaced by the best tested mirror mount except those of the laser pump mirror and the two deflection mirrors of the fiber coupling which are motorized to compensate tilts of other mirrors. The tuning mirror is not motorized anymore and hence more stable but a tuning of the wavelength via the etalon will result in a reduced output power. The dependence of the wavelength from the pressure is eliminated by replacing the air-spaced etalon by a solid etalon and mounting the dispersion prisms within an airtight housing and hence a filling of the resonator volume with helium is unnecessary. Furthermore the NLO oven is mounted fix on the baseplate and its angle is no longer adjustable. A tilt of the crystal is avoided and the phase matching is achieved by changing the temperature online.

### 3.2 Laser Performance in the laboratory

The laser is characterized under laboratory conditions and fulfills all requirements derived from the LIF measurement as shown in Table 3.

Table 3. Required and achieved parameters of the laser in the laboratory.

parameter	requirement	achieved
central wavelength	308,160 nm	308,160 nm
tuning range	100 GHz	> 100 GHz
linewidth	< 7 GHz	6 GHz
wavelength stability	1 pm	< 1 pm
power within tuning range	50 - 100 mW	150 - 180 mW
power stability	< 20 %	5 %
M <sup>2</sup> of fundamental	--	1,4
pulse repetition rate	8500 Hz	8500 Hz
pulse duration	< 30 ns	21 ns

The wavelength is determined by the angle of the etalon as shown on the left side of Figure 7. The etalon is mounted in such a way that the turning point is right at the upper limit of the demanded tuning range around the central wavelength.

Thereby the output power is over 150 mW for the whole tuning range and the wavelength can be controlled with a high resolution.

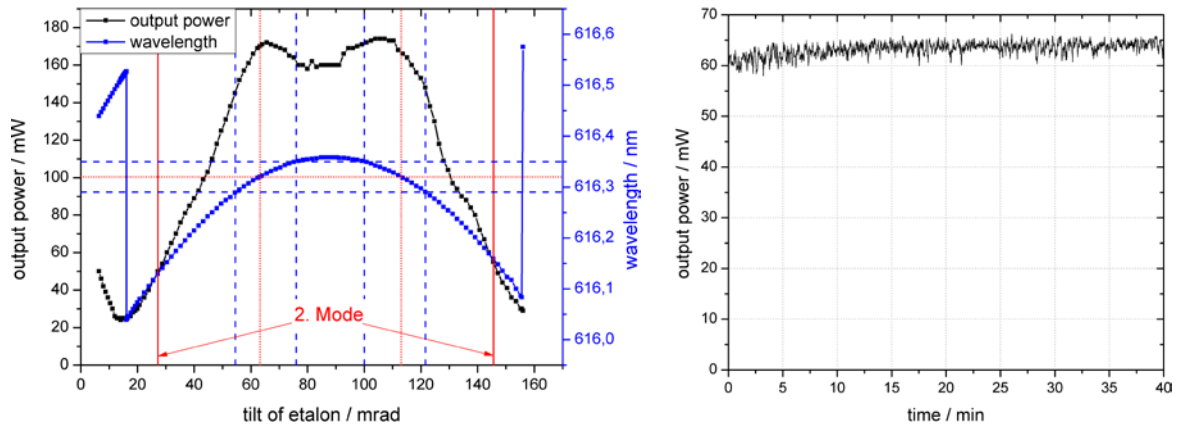


Figure 7. Output power and wavelength of the UV laser in dependence of the tilt of the etalon (left) and output power stability behind the first fiber (right).

The power stability behind the first fiber where 50 % of the power is coupled in is shown on the right side of Figure 7. Within a period of 40 minutes the fluctuations are smaller than 5 %.

The laser worked over 600 operation hours before the dye and some optics were replaced.

### 3.3 Airborne Laser Performance

Two successful field campaigns in the Netherlands and northern Italy were carried out over a period of seven weeks with the redesigned laser. Daily interruption-free measurements lasting for several hours were performed without any readjustment or maintenance of the laser.

However the output power is not as stable as shown in the lab. On the left side of Figure 8 the output power and the temperature of the box in which the laser was mounted are shown. The fluctuations of the output power are up to 30 % and follow the form of the temperature even though the changes are only 0.5 °C. Since the power was sufficient for the measurement the temperature of the NLO crystal was not altered though it might have restored the output power.

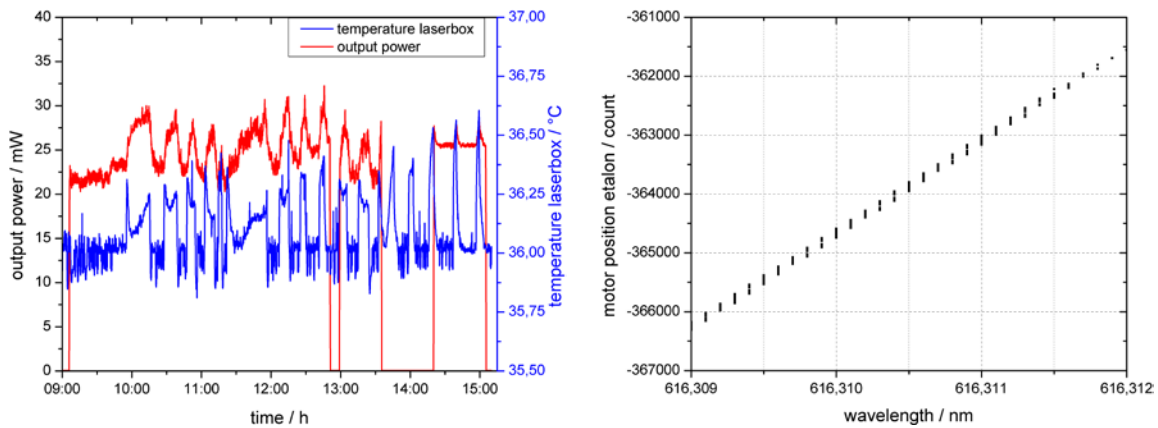


Figure 8. Output power of the UV laser and temperature of the laserbox over the time (left) and dependence of the wavelength on the motor position (right) (both from [10]).

On the right side of Figure 8 the wavelength for each motor position accumulated over a day is shown. The laser emits always at the same wavelength for a certain motor position despite changing ambient pressure and temperature. The discrete distribution comes from the resolution of the spectrometer used for the measurement. Thereby the wavelength stability and the independence from ambient pressure are reached.

#### 4. DESIGN IMPROVEMENTS FOR FUTURE MISSIONS

For future missions several improvements of the optical and mechanical design are worthwhile. The temperature control of the box in which the laser is installed and of the laser baseplate itself has to be improved for a more stable temperature and hence less misalignments of the mounts. The changes of the pump laser pointing can be compensated by active beam stabilization ensuring a good overlap with the laser mode.

The conversion efficiency can be optimized by an active control of the NLO crystal temperature to compensate given tilts of the laser mode. It can be further increased by using an AR-coated crystal instead of a Brewster-cut crystal because internal reflection of the converted light is prevented. Also it is worth to test alternative lengths of the crystal to meet to optimal output coupling for the laser and guarantee a more stable operation point. To increase the lifetime of the optics and the dye an additional folding of the resonator between the dye cell and the NLO crystal can minimize the number of optics that is UV-loaded.

#### 5. SUMMARY

In this work, a detailed analysis and redesign of a tunable UV laser for the airborne LIF measurements of the OH-radical concentration was presented. The analysis of the existing laser combined theoretical study of tolerance requirements with experimental testing of opto-mechanical components and of the entire laser system in a climatic chamber. The theoretical study identified the most critical optics and quantified the tolerance for tilts and displacements. The measurements in the climatic test chamber demonstrated that the up to now used mounts are 50 times more susceptible to temperature changes than the best alternative mount tested. The test with the whole laser system showed that changing the baseplate temperature by few Kelvin stops laser emission completely.

A new laser has been built based on the results of the analysis and further experiments for an optical redesign. This laser meets all requirements and was successfully deployed during the PEGASOS field campaigns in 2012.

#### REFERENCES

- [1] Holland, F., Hessling, M. and Hofzumahaus, A., "In-Situ Measurement of Tropospheric OH Radicals by Laser-Induced Fluorescence -A Description of the KFA Instrument," *J. Atmos. Science* 52, 3393-3401 (1995).
- [2] "PEGASOS", < <http://pegasos.iceht.forth.gr> > (25 January 2013)
- [3] Hofzumahaus, A.; Holland, F., "Zeppelin NT, a new Platform for Atmospheric Studies in the Planetary Boundary Layer.", Forschungszentrum Jülich, (2006)
- [4] Wennberg, P. O., Cohen, R.C., Hazen, N.L., Lapson, L.B. and Allen, N.T., "Aircraft-borne, laser induced fluorescence instruments for the in-situ detection of hydroxyl and hydroperoxyl radicals," *Rev. Sci. Instrum.* 65, 1858-1876 (1994).
- [5] Faloon, I.C., Tan, D., Leshner, R.L., Hazen, N.L., Frame, C.L., Simpas, J.B., Harder, H., Martinez, M., Di Carlo, P., Ren, X. and Brune, W.H., "A Laser-induced Fluorescence Instrument for Detecting Tropospheric OH and HO<sub>2</sub>: Characteristics and Calibration," *Journal of Atmospheric Chemistry* 47, 139-167 (2004).
- [6] Martinez M., Harder, H., Kubistin, D., Ridolf, M., Bozem, H., Eerdeken, G., Fischer, H., Klüpfel, T., Gurk, C., Königstedt, R., Parchatka, U., Schiller, C.L., Stickler, A., Williams, J. and Lelieveld, J., "Hydroxyl radicals in the tropical troposphere over the submarine rainforest: airborne measurements," *Atmospheric Chemistry and Physics* 10, 3759-3773 (2010).
- [7] Matsumi, Y., Kono, M., Ichikawa, T., Takahashi, K. and Kondo, Y., "Laser-Induced Fluorescence Instrument for the Detection of Tropospheric OH Radicals," *Bulletin of the Chemical Society of Japan* 75(4), 711-717 (2002).

- [8] Siegmann, A. E., [Lasers], University Science Books, (1986)
- [9] Boyd, R. W., [Nonlinear Optics], Academic Press, San Diego, (1992)
- [10] Holland, F., private communication, (2012)